

# Measurements of Correlation-Enhanced Collision Rates

Francois Andereg, Daniel H. E. Dubin, Thomas M. O’Neil  
and C. Fred Driscoll

*Department of Physics, University of California at San Diego, La Jolla, CA USA 92093-0319*

**Abstract.** We present the first detailed experimental measurements of the Salpeter collisional enhancement factor in correlated plasma. This factor is predicted to enhance the nuclear reaction rate in dense correlated plasmas such as in giant planet interiors, brown dwarfs and degenerate stars. Recent non-neutral plasma theory establishes that it also applies to the perpendicular-to-parallel collisions in magnetized plasmas. The enhancement is caused by plasma screening of the repulsive Coulomb potential between charges, allowing closer collisions for a given particle energy. The enhancement factor is large when the plasma correlation factor  $\Gamma$  is larger than unity, scaling as  $g(\Gamma) \simeq e^\Gamma$ . We perform measurements of collision rate in laser-cooled magnesium ion plasmas with density  $n \sim 10^7 \text{ cm}^{-3}$  and temperature  $2.5 \times 10^{-6} < T < 1 \text{ eV}$ , resulting in  $0 < \Gamma < 25$ . We observe that at high  $\Gamma$  (i.e. low temperature), the collision rate is increased by a factor up to  $10^9$  over the uncorrelated theory prediction, consistent with the Salpeter enhancement.

**Keywords:** collision, correlation, nonneutral plasma

**PACS:** 52.20Hv, 52.27Jt, 52.27Gr, 24.10Pa

## INTRODUCTION

We present theory results and measurements that use non-neutral plasmas to model aspects of the physics of nuclear fusion reactions in dense, correlated plasmas, such as in giant planets, degenerate stars, and laser fusion plasmas. Nuclear reaction rates in dense correlated plasmas are, according to theory, enhanced compared to rates predicted for reactions at lower density. In the astrophysics community, this theoretical effect is known as the Salpeter enhancement [1]. Here we use an analogy between screened nuclear reactions in dense plasmas and perpendicular-to-parallel energy equipartition in strongly coupled and strongly magnetized non-neutral plasmas [2, 3].

In a magnetized plasma with a perpendicular temperature  $T_\perp$  and a parallel temperature  $T_\parallel$ , we consider the perpendicular-to-parallel collision rate  $\nu_{\perp\parallel}$  defined as:

$$\frac{d}{dt} T_\perp = \nu_{\perp\parallel} (T_\parallel - T_\perp), \quad \text{with} \quad (1)$$

$$\nu_{\perp\parallel} \equiv n \bar{v} b^2 4\sqrt{2} I(\bar{\kappa}) g(\Gamma). \quad (2)$$

Here, the “bare” collision rate  $4\sqrt{2} n \bar{v} b^2$  is modified by a dynamical factor  $I(\bar{\kappa})$ , depending only on the magnetization parameter

$$\bar{\kappa} \equiv \sqrt{2} b/r_c;$$

and modified by an equilibrium correlation factor  $g(\Gamma)$ , depending only on the correlation parameter

$$\Gamma \equiv e^2/aT .$$

(All symbols are defined below.) Laser cooling enables ion plasma equilibria well into the cryogenic regime, with  $T = 1\text{eV} \rightarrow 10^{-5}\text{eV}$ , resulting in  $I(\bar{\kappa}) \approx 2 \rightarrow 10^{-5}$  and  $g(\Gamma) \approx e^\Gamma \approx 1 \rightarrow 10^9$ . The measured  $v_{\perp\parallel}$  agree quantitatively with standard collisional theory in the high temperature plasma regime; and agree quantitatively with the adiabatic invariant prediction for magnetization suppression  $I(\bar{\kappa})$ ; and are consistent with the ‘‘equilibrium’’ Salpeter enhancement for weak correlations  $\Gamma \lesssim 10$ . Moreover, the measured collision rates show the expected independence of the dynamical parameter  $\bar{\kappa}$  from the equilibrium parameter  $\Gamma$ .

## THEORY

The theory of collisions in strongly magnetized plasma was developed by O’Neil and colleagues [4, 5], with theory and simulations spanning the full range of magnetization. Separately, the equilibrium theory of correlation-enhanced collisions was developed by Salpeter [1]; and was adapted to magnetized plasmas by Dubin [3].

Here, we briefly review the results using the perspective and notation of Ref. [3], that is, using CGS units and expressing temperature in units of energy. The (single component) plasma equilibrium has density  $n$  and temperature  $T$ , giving thermal velocity  $\bar{v} \equiv (T/m)^{1/2}$ , distance of closest approach  $b \equiv e^2/T$ , and interparticle spacing  $a \equiv (3/4\pi n)^{1/3}$ . Magnetization gives dynamical parameters  $\Omega_c \equiv eB/mc$  and  $r_c \equiv \bar{v}/\Omega_c$ .

The perpendicular-to-parallel collision rate of Eq. (2) represents an integral over the relative velocities of colliding particles. In the ‘‘normal’’ plasma regime ( $T > 10^{-2}\text{eV}$ ,  $r_c \gg b$ ,  $\bar{\kappa} \ll 1$ ,  $\Gamma \ll 1$ ), integration gives the ‘‘classical’’ result

$$I(\bar{\kappa}) = \frac{\sqrt{2\pi}}{15} [\ln(r_c/b) + 0.75] , \quad g(\Gamma) = 1 , \quad (3)$$

resulting in the ‘‘normal’’ nonneutral plasma collision rate

$$v_{\perp\parallel} = n\bar{v}b^2 \frac{8\sqrt{\pi}}{15} [\ln(r_c/b) + 0.75] \propto nT^{-3/2}. \quad (4)$$

The enhancement of 0.75 is obtained in Ref. [5].

### Strong Magnetization

At lower temperatures ( $T < 10^{-3}\text{eV}$ ), the cyclotron radius  $r_c$  becomes comparable to the distance of closest approach  $b$ , and the collision time  $\tau_{\parallel} \equiv b_{\parallel}/v_{\parallel}$  becomes large compared to  $\Omega_c^{-1}$ . A two-particle adiabatic invariant  $E_{\perp} \equiv E_{\perp 1} + E_{\perp 2}$  then constrains the collision dynamics and decreases  $v_{\perp\parallel}$ . The collision integral can then be expressed

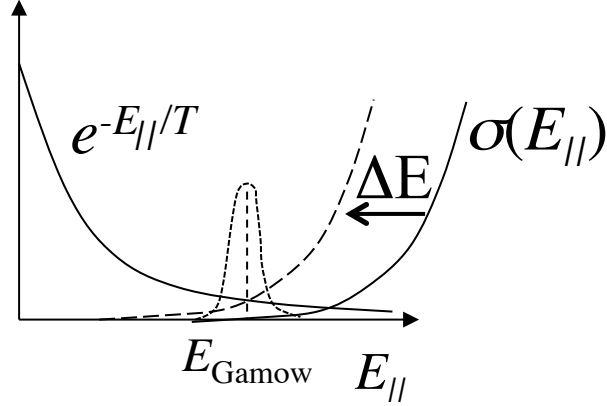


**FIGURE 1.** Graphic description of the integrand of Eq. (5) showing exponentially decaying Maxwellian particle energy distribution and the exponentially growing cross-section  $\sigma$ . The product of the particle distribution and the cross-section gives rise to the Gamow peak. Shifting  $\sigma$  by  $\Delta E$  gives enhancement  $\exp(\Delta E/T)$ .

as the product of a Maxwellian with the dynamical cross-section  $\sigma(E_{\parallel})$ , as

$$v_{\perp\parallel} = \int \frac{dE_{\parallel}}{T} \exp\left(\frac{-E_{\parallel}}{T}\right) \sigma(E_{\parallel}) , \text{ with} \quad (5)$$

$$\sigma(E_{\parallel}) \propto e^{-\pi\Omega_c\tau_{\parallel}} \propto e^{-(\pi c/E_{\parallel})^{3/2}} . \quad (6)$$

The integrand peaks at the Gamow energy  $E_G \equiv 1.23(\bar{\kappa})^{2/5}T$ , as shown in Fig. 1, and various approximate expressions have been obtained for  $I(\bar{\kappa})$ . In the regime of interest here,

$$v_{\perp\parallel}^{\text{no corr}} = n\bar{v}b^2 4\sqrt{2} I(\bar{\kappa}) \quad (7)$$

with

$$I(\bar{\kappa}) \approx c e^{-2.044(\bar{\kappa})^{2/5}} \quad (8)$$

where  $c \simeq 1.5$  in the regime of interest.

The collision rate in this regime was measured in a pure electron plasma contained in a cryogenic apparatus [6]. Figure 2 shows the measured collision rate plotted versus temperature (lower axis) and versus  $\bar{\kappa}$  (upper axis); the collision rate is strongly suppressed as  $\bar{\kappa}$  gets larger than 1. It is worth noting that particles contributing to the collision rate are at energy  $E_{\text{Gamow}} = 1.23\bar{\kappa}^{2/5}T$ , for a value of  $\bar{\kappa} = 20$ ; this corresponds to particles of velocity  $4\bar{v}$ , that is, less than 2% of the particles participate in such (rare) collisions. Here the cyclotron energy is released only by rare energetic collisions, similarly in nuclear fusion reactions where the energy stored in the nuclei is liberated only by rare energetic collisions.

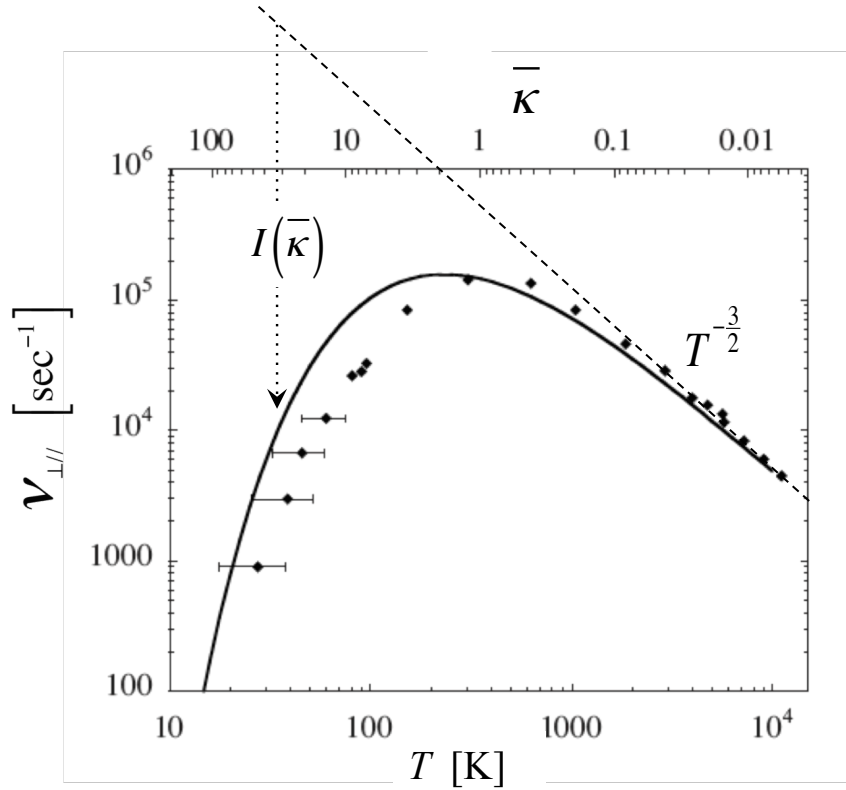


**FIGURE 2.** Adapted from Ref. [6]. Collision rate versus temperature (lower axis) and  $\bar{\kappa}$  (upper axis) for an uncorrelated pure electron plasma with  $B = 6.13T$ ,  $n = 8 \times 10^8 \text{ cm}^{-3}$ . The solid theory curve is Eq. (7), the  $T^{-3/2}$  scaling of Eq. (4) is shown with the long dashed line, and the strong magnetization suppression  $I(\bar{\kappa})$  in the collision rate of Eq. (8) is shown by the arrow.

## Correlations

Correlations enhance the perpendicular-to-parallel collision rate through screening effects, by reducing the amount of parallel energy required by two ions to come within a distance  $\rho$ . In the absence of shielding the energy required is  $E_{\parallel} = e^2/\rho$ ; in contrast, with Debye screening the parallel energy required is smaller:  $E_{\parallel} = (e^2/\rho) \exp(-\rho/\lambda_D) \simeq e^2/\rho - e^2/\lambda_D$ . In other words, screening reduces the parallel energy required to come within a distance  $\rho$ .

In the strong coupling regime of  $\Gamma > 1$ , the effective shielding distance is the inter-particle spacing, and the energy required for a collision at distance  $\rho < a$  is

$$E_{\parallel} = \frac{e^2}{\rho} - \frac{e^2}{a}. \quad (9)$$

This shifts  $\sigma(E_{\parallel})$  by  $e^2/a$ , as shown in Fig. 1. Equivalently, the Maxwellian in Eq. (4) is shifted by  $\Delta E_{\parallel}/T = e^2/aT = \Gamma$ ,

$$\begin{aligned} v_{\perp\parallel}^{\text{corr}} &= \int dE_{\parallel} \frac{1}{T} \exp\{-(E_{\parallel} - e^2/a)/T\} \sigma(E_{\parallel}) \\ &= \exp\left(\frac{e^2}{aT}\right) \int dE_{\parallel} \frac{1}{T} \exp\left(-\frac{E_{\parallel}}{T}\right) \sigma(E_{\parallel}) \\ &= \exp(\Gamma) v_{\perp\parallel}^{\text{no corr}}; \end{aligned} \quad (10)$$

giving a collisional enhancement over the non-correlated case:

$$g(\Gamma) = e^{\Gamma}. \quad (11)$$

Thus the perpendicular-to-parallel collision rate is enhanced by correlation by a factor  $g = \exp(\Gamma)$ . More precise ‘‘equilibrium shielding’’ calculations of  $g(\Gamma)$  have been performed [3, 7, 8], giving results essentially identical to Eq. (11) within our experimental range. It is worth noting that the enhancement is independent of  $\sigma(E)$ , as in the fusion case, where this effect is known as the Salpeter enhancement.

It is interesting to note that the inside of a giant planet has a temperature  $T \sim 1\text{eV}$  and a density  $n \sim 10^{24}\text{cm}^{-3}$  resulting in  $\Gamma \sim 10$ ; also, white dwarf stars have typical temperature  $T \sim 100\text{eV}$  and density  $n \sim 10^{30}\text{cm}^{-3}$ , also resulting in  $\Gamma \sim 10$  [9]. At present, our sun has a small coupling parameter  $\Gamma = 0.05$ , having only a small effect on the fusion rate of the sun ( $g \simeq 1.05$ ). Laser cooled ion plasmas can easily have  $T \sim 10^{-5}\text{eV}$  and  $n \sim 2 * 10^7\text{cm}^{-3}$  also resulting in  $\Gamma \sim 10$ . A non-neutral plasma can be used to study the properties of astrophysical objects as long as the physical process depends on the coupling parameter  $\Gamma$ .

## EXPERIMENTS

To test the theoretically predicted correlation enhancement of the collision rate, we use a magnesium ion plasma contained in a Penning-Malmberg trap. A description of the apparatus can be found in Ref. [10]. The plasma density for this experiment is controlled with a rotating wall ( $0.12 \times 10^7 \leq n \leq 2 \times 10^7\text{cm}^{-3}$ ), the temperature is controlled by laser cooling ( $2.5 \times 10^{-6}\text{eV} < T < 1\text{eV}$ ), the uniform axial magnetic field was changed in the range of  $1.2T \leq B \leq 3T$ . The plasma radius is  $R_p \simeq 0.5\text{cm}$  and the plasma length is  $L_p \simeq 10\text{cm}$ . The adiabaticity parameter is  $\bar{\kappa} = 1$  at a temperature  $T = 5 \times 10^{-4}\text{eV}$  and  $B = 3T$ . The coupling parameter is  $\Gamma = 1$  for  $n = 2 \times 10^7\text{cm}^{-3}$  and  $T = 6 \times 10^{-5}\text{eV}$ .

We use two different techniques to measure the perpendicular-to-parallel collision rate  $v_{\perp\parallel}$ . The first technique directly observes  $T_{\perp}$  and  $T_{\parallel}$  as they relax to a common temperature. The parallel temperature is initially increased by small oscillating voltages applied at one end of the plasma. This causes a variation of the plasma length  $\Delta L$ , with a consequent variation  $\Delta T_{\parallel}/T \propto (\Delta L/L)^2$ , resulting in  $T_{\parallel} > T_{\perp}$ . This direct measurement is practical only for slow rates ( $v_{\perp\parallel} < 100\text{s}^{-1}$ ) and is not accurate for low temperature  $T < 10^{-4}\text{eV}$  since ion-neutral collisions give a heating rate which dominates the temperature evolution.

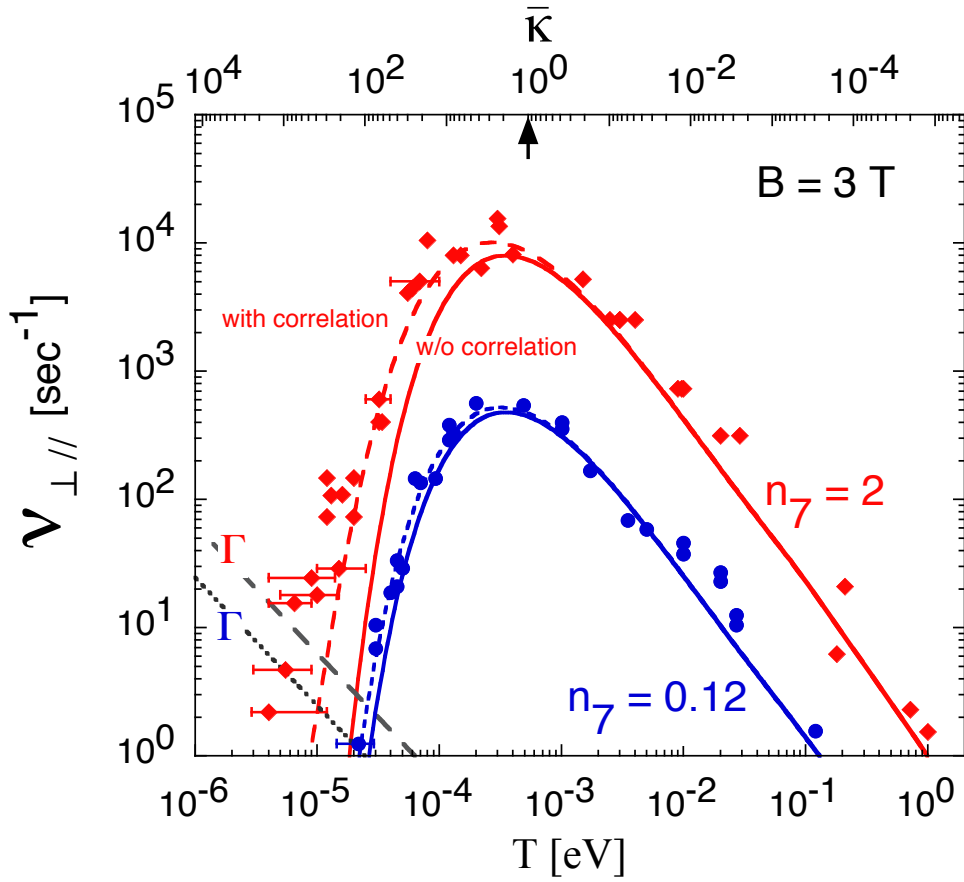


**FIGURE 3.** Measured collision rates for two densities versus temperature (lower axis) and  $\bar{k}$  (upper axis) compared to theory with and without correlations. The correlation parameter  $\Gamma$  for high and low density is also shown.

The second technique obtains  $v_{\perp\parallel}$  by determining the frequency  $f_{\text{osc}}$  at which axial compressions give maximum heating [6]. A short oscillating burst (3  $\rightarrow$  100 cycles) at frequency  $f_{\text{osc}}$  is applied to one cylindrical electrode at one end of the plasma. The heating due to the burst is maximal when  $v_{\perp\parallel} = c(\Gamma)2\pi f_{\text{osc}}$  where  $c(\Gamma)$  is the specific heat  $c(\Gamma) = c_{\parallel}c_{\perp}/(c_{\parallel} + c_{\perp})$  with  $c_{\perp} = 1$  and  $c_{\parallel} = 1/2 + \partial U_{\text{corr}}/\partial T$ ; the correlation energy  $U_{\text{corr}}$  is defined by Eq. (4.24) in Ref. [11]. The specific heat increases slowly with correlation, with  $c(0) = 1/3$ ,  $c(2) \simeq 0.42$  and  $c(10) \simeq 0.52$ .

The measured perpendicular-to-parallel collision rate is plotted in Fig. 3 for two densities,  $n = 2 \times 10^7$  and  $0.12 \times 10^7 \text{ cm}^{-3}$  labeled  $n_7 = 2$  and  $n_7 = 0.12$ . In both cases the collision rate is strongly suppressed when  $\bar{k}$  is larger than unity. The solid lines are theory curves obtained from Eq. (7) using numerical values of  $I(\bar{k})$  from Ref. [5], with no adjustable parameters. The dashed lines are from Eq. (10). At lower density the plasma is never strongly correlated, as shown by  $\Gamma$  which is also plotted for both densities. The  $n = 2 \times 10^7 \text{ cm}^{-3}$  density data (labeled  $n_7 = 2$ ) have  $\Gamma > 1$  at low temperatures, and the measured collisionality is enhanced by several orders of magnitude over theory neglecting correlations. At low density, the collision rate is measured down to a rate of  $1 \text{ sec}^{-1}$ , setting an upper limit on extraneous collisional effects. Figure 4 shows the

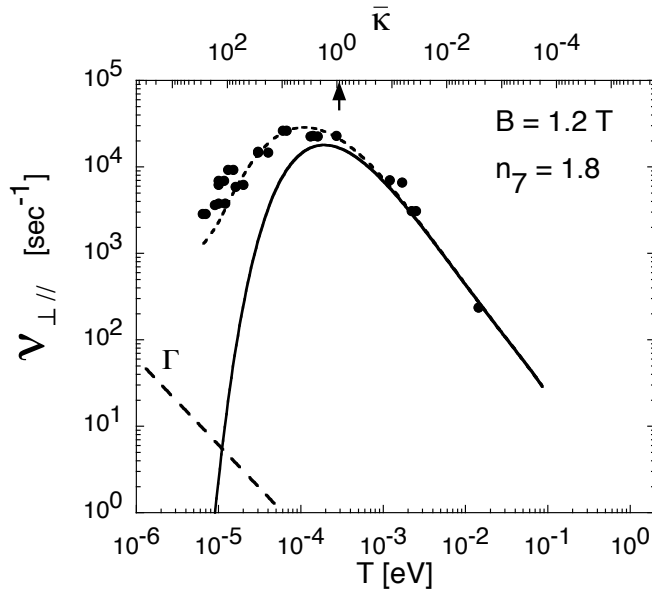


**FIGURE 4.** Same as Fig. 3 but for lower magnetic field. The  $I(\bar{\kappa})$  suppression is less in the  $\Gamma > 1$  regime resulting in higher collision rate.

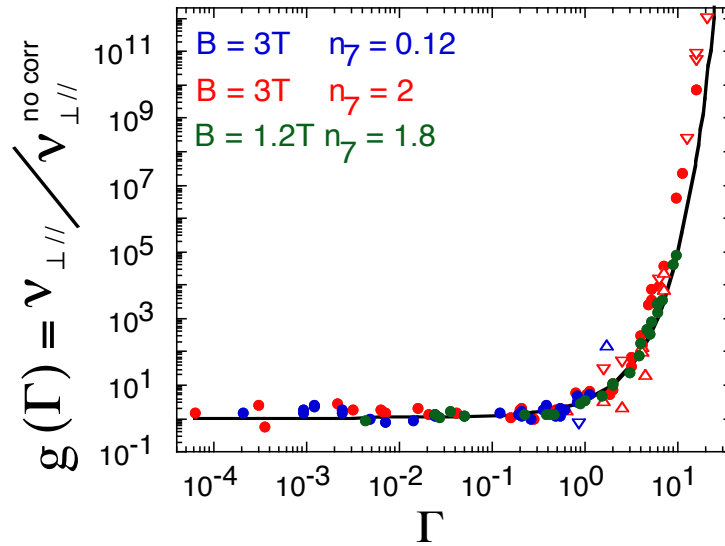


**FIGURE 5.** Measured enhancement  $g(\Gamma)$  for all the data of Figs. 3 and 4, demonstrating that  $g(\Gamma) \simeq \exp(\Gamma)$  is independent of  $\bar{\kappa}$ . The theory line is from Eq. (11).

measured collision rate at a lower magnetic field  $B = 1.2T$ . The correlation parameters  $\Gamma$  and  $g(\Gamma)$  are independent of the magnetic field; in contrast  $\bar{\kappa}$  depends on the magnetic field. Therefore the  $I(\bar{\kappa})$  suppression is less in the  $\Gamma > 1$  regime, resulting in higher collision rates in the correlated regime. Here also the solid line is from Eq. (7) and the dashed line from Eq. (10).

Figure 5 shows the measured collision rate divided by the theoretical rate neglecting correlations, that is, the Salpeter enhancement  $g(\Gamma)$ . The enhancement depends on  $\Gamma$  but is independent of  $\bar{\kappa}$ , as predicted by theory. The measured correlation enhancement  $g(\Gamma)$  is consistent with “equilibrium shielding” theories, and no support for alternative “dynamic shielding” effects is seen. This work illustrates how laboratory non-neutral plasmas can be used to study high energy density plasmas where the same enhancement applies to rare energetic fusion collisions in hot, dense correlated plasmas such as stars.

## ACKNOWLEDGMENTS

This work was supported by National Science Foundation Grant No. PHY0903877 and Department of Energy Grants DE-SC0002451 and DE-SC0008693.

## REFERENCES

1. E. E. Salpeter, *Aust. J. Phys.* **7**, 373 (1954); E. E. Salpeter and H. Van Horn, *Astrophys. J.* **155**, 916 (1969).
2. F. Andereg, D. H. E. Dubin, T. M. O’Neil and C. F. Driscoll, *Phys. Rev. Lett.* **102**, 185001 (2009); F. Andereg, C. F. Driscoll, D. H. E. Dubin and T. M. O’Neil, *Phys. Plasmas* **17**, 055702 (2010).
3. D. H. E. Dubin, *Phys. Plasmas* **15**, 055705 (2008); D. H. E. Dubin, *Phys. Rev. Lett.* **94**, 025002 (2005).
4. T. M. O’Neil and P. G. Hjorth, *Phys. Fluids* **28**, 3241 (1985).
5. M. E. Glinsky and T. M. O’Neil, *Phys. Fluids B* **3**, 1279 (1991).
6. B. R. Beck, J. Fajans and J. H. Malmberg, *Phys. Plasmas* **3**, 1250 (1996).
7. S. Ogata, *Astrophys. J.* **481**, 833 (1997).
8. H. DeWitt and W. Slattery, *Contrib. Plasma Phys.* **39**, 97 (1999).
9. *Frontiers in High Energy Density Physics*, The National Academic Press, Washington DC (2003).
10. F. Andereg, X.-P. Huang, E. Sarid, and C. F. Driscoll, *Rev. Sci. Instrum.* **68**, 2367 (1997).
11. D. H. Dubin and T. M. O’Neil, *Rev. Mod. Phys.* **71**, 87 (1999).